ELSEVIER

Ceramics International 31 (2005) 297–303

CERAMICS INTERNATIONAL

www.elsevier.com/locate/ceramint

Characteristics of yttria stabilized tetragonal zirconia powder used in optical fiber connector ferrule

Chih-Liang Yang[a], Hsing-I. Hsiang[a,*], Chih-Cheng Chen[b]

[a]*Department of Resources Engineering, National Cheng-Kung University, Tainan, Taiwan, ROC*
[b]*Department of Mechanical Engineering, Far East College, Tainan, Taiwan, ROC*

Received 4 December 2003; received in revised form 9 March 2004; accepted 10 May 2004
Available online 25 August 2004

Abstract

The tetragonal to monoclinic (t → m) phase transformation during low temperature (~100 °C) degradation (LTD) of yttria-stabilized tetragonal zirconia polycrystals (Y-TZP) sintered in air at different temperatures was investigated. It is found that the sintering temperature affected the density, crystalline phase and microstructure of the sintered body, as well as the LTD behavior. Also, the onset time of the occurrence of m-ZrO_2 in the annealed samples during LTD was longer than the unannealed samples.

Keywords: A. Sintering; Yttria-stabilized tetragonal zirconia polycrystals; Low temperature degradation; Phase transformation

1. Introduction

Yttria tetragonally stabilized zirconia (Y-TZP) is of great interest due to its high strength, high toughness, chemical stability, high melting temperature, ionic, electrical and optical properties in advanced ceramics. They are widely used as wear resistant components, solid state electrolyte and optical fiber connectors, like ferrules.

The ferrule materials should satisfy a set of conditions, such as stability during environmental changes, thermal expansion coefficient and hardness close that of SiO_2 glass, low Young's modulus, and good-quality polished surface. Since Y-TZP satisfies the above requirements, it is generally selected for making ferrules. Y-TZP is stable up to 2370 °C, but aging at temperatures between 100 and 300 °C in the presence of water could severely degrade the properties. Several mechanisms of low temperature degradation (LTD) have been proposed; however, most of them were only concerned about fracture strength and toughness. The most well known LTD work was performed by Lange [1] in which the degradation of the sintered, polycrystalline Y-TZP with yttrium content ranging from 2 to 6 mol% at 250 °C in a humid environment was investigated. They concluded that the tetragonal grains were attacked by water on the surface of the ceramic. They hypothesized that water leached a sufficient amount of yttrium such that the surface tetragonal grains transformed into the monoclinic phase. Further depletion of yttrium caused the monoclinic structure to grow until a critical size was reached. At this critical size, the t → m-ZrO_2 transformation occurred spontaneously and resulted in the formation of micro- and macro-cracks. Furthermore, Kimel and Adair also showed that t → m phase transformation decreased with increasing yttrium content [2]. Li et al. [3] investigated the LTD behavior of 2 and 3 mol% Y_2O_3-ZrO_2 ceramics and their composites with the addition of 5 vol.% Al_2O_3 in water and vacuum at 353–623K. They found that t → m phase transformation during annealing in water was dominated by H_2O at lower temperature and was dominated by thermal activation at higher temperature. Guo [4] proposed a new mechanism for the degradation phenomenon, in which the oxygen vacancies are considered to play a decisive role. Although the details of the new mechanism need to be elaborated by further studies, the new mechanism has satisfactorily

* Corresponding author. Tel.: +886 6 2757575x62821; fax: +886 6 2380421.
E-mail address: hsingi@mail.ncku.edu.tw (H. Hsiang).

0272-8842/$30.00
doi:10.1016/j.ceramint.2004.05.020

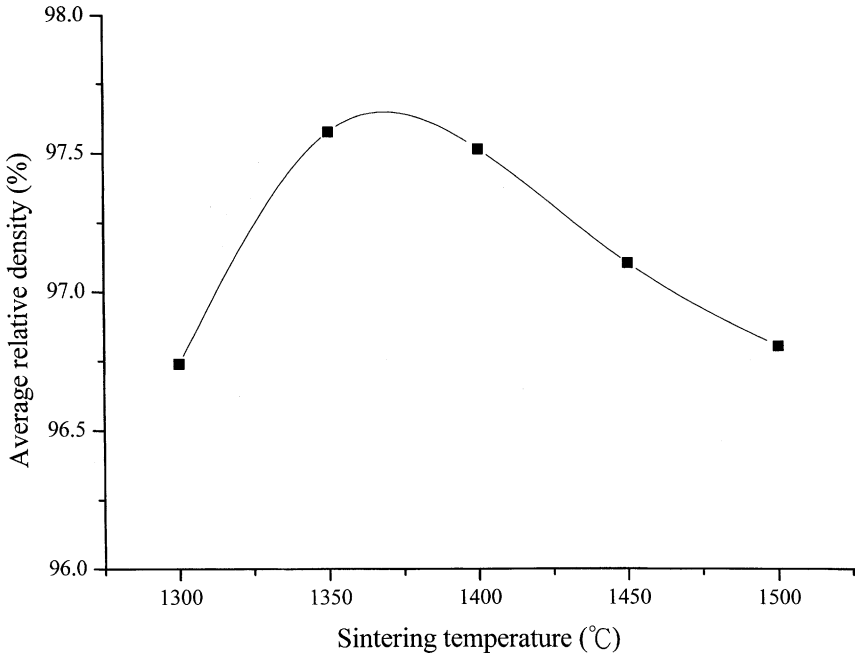

Fig. 1. The relative density of Y-TZP at different sintering temperatures.

explained most phenomenological observations concerning the degradation.

Preparing the ferrule used in the optical fiber connector usually requires polishing treatment, which concerns more on the extremely high dimensional tolerance and high quality polished surface than on the fracture strength and toughness. However, previous reports mostly focused on the effects of LTD on the t → m-ZrO_2 transformation and fracture strength of the sintered surface for Y-TZP. [5-7] Therefore, this study investigated the kinetics of sintering and the effects of polishing and annealing treatments on the LTD behavior of Y-TZP.

2. Experimental procedure

The commercially available zirconia powder (3-YE, Tosoh, Japan) was used in the present study. The disk-

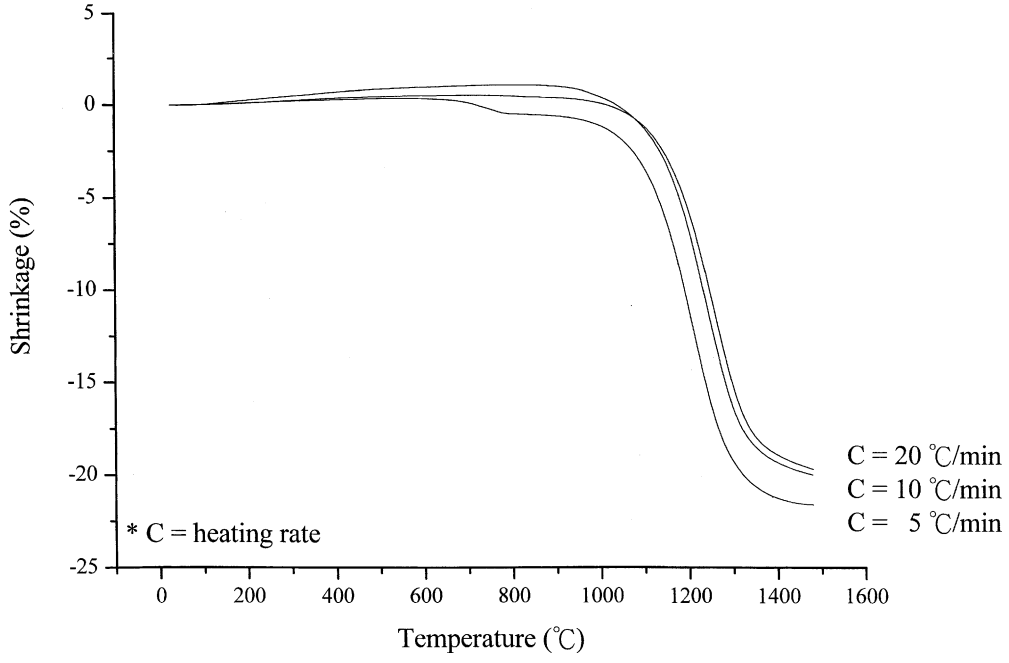

Fig. 2. The linear shrinkages vs. sintering temperatures at different heating rates.

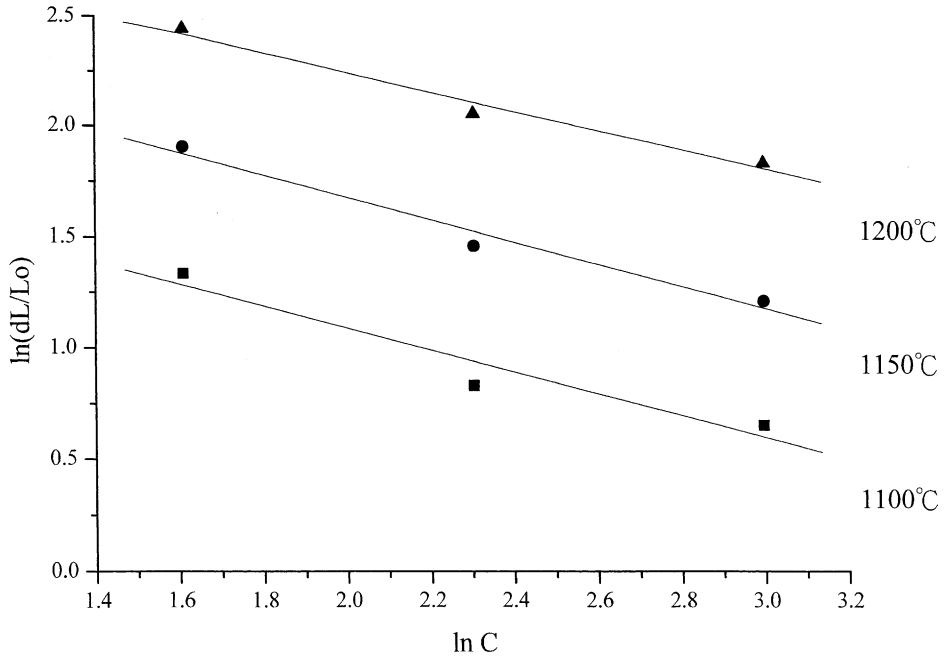

Fig. 3. A plot of $\ln(dL/L_0)_T$ vs. $\ln(C)$ for 3-YE.

shaped YTZP was formed by die-pressing at 0.8 t followed by cold isostatic pressing at 200 MPa. The green compacts were sintered in air at 1300, 1350, 1400, 1450, 1500 °C for 2 h, respectively, and then cooled in a furnace. After sintering, the disk was polished using diamond paste and then annealed for 30 min at 1200 °C. The apparent density was measured by the Archimedes method, and the relative density was calculated using the theoretical density of 6.10 g/cm^3. The aging treatments were carried out in water at 100 °C for 2, 5, 10, 20, 50 h, respectively. Aged samples were analyzed by XRD and SEM to observe the phase transformation and low temperature degradation behaviors. Besides, the sintering studies were performed by a dilatometer (DIL) in which the samples were heated at a constant rate of 5, 10 and 20 °C/min to 1500 °C.

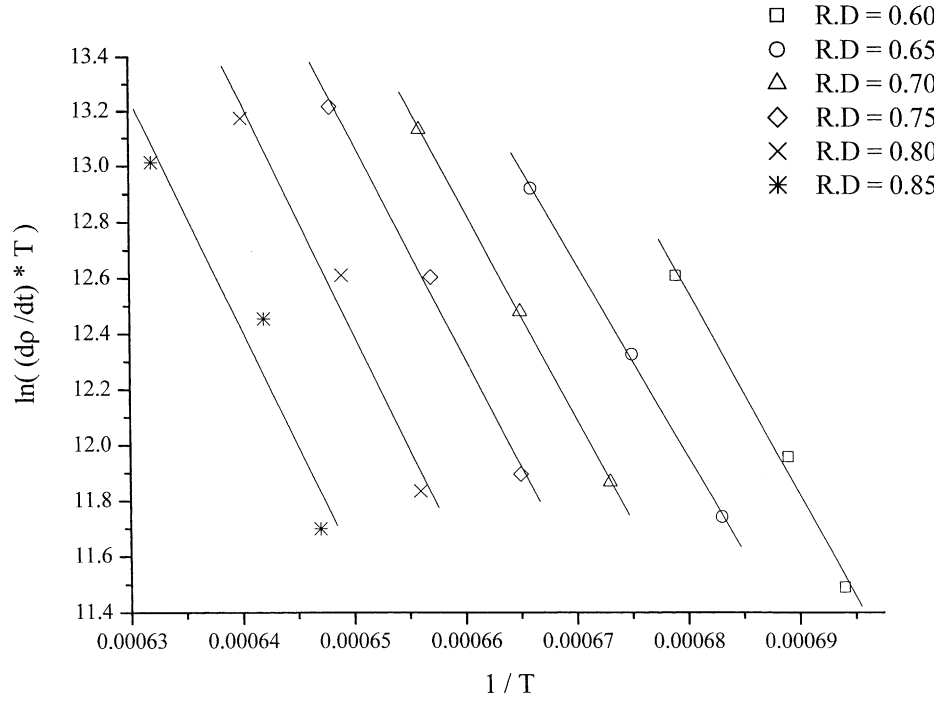

Fig. 4. Arrhenius plots for the densification at different heating rates.

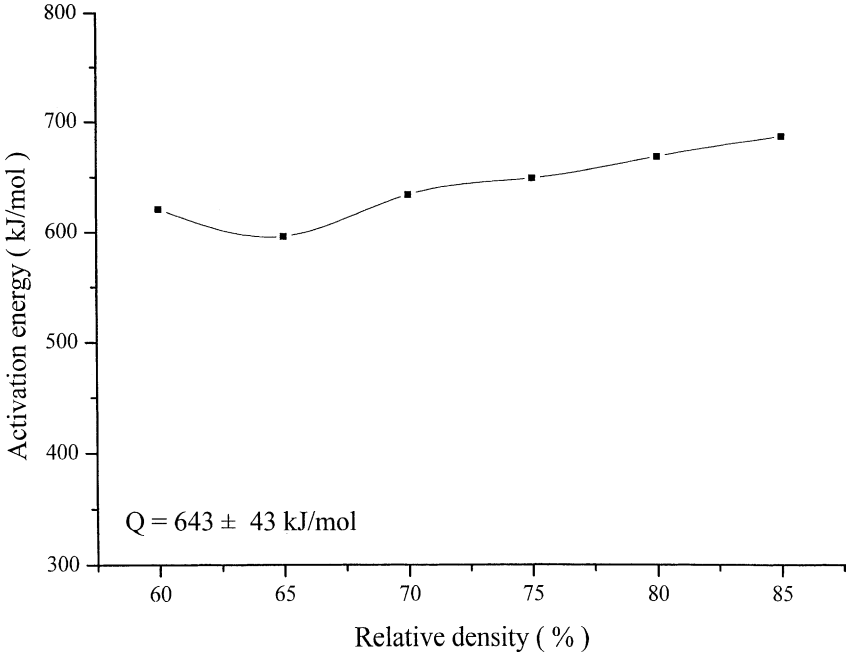

Fig. 5. The calculated values of the activation energy for 3-YE.

3. Results and discussion

3.1. Sintering behavior

Fig. 1 shows that the relative density of Y-TZP increased with increasing sintering temperature. The relative density reached the maximum (about 97%) at 1350 °C, and then decreased with increasing temperature.

This study used a DIL to analyze the densification behavior of 3-YE disk. The specimens were sintered up to 1500 °C by using three different heating rates, i.e., 5, 10 and 20 °C/min. The densification curves were plotted in Fig. 2. It shows that the densification curves of 3-YE were shifted to higher temperatures and had less shrinkage as the heating rate was increased. Among the samples with three different heating rates, the shrinkage of the sample

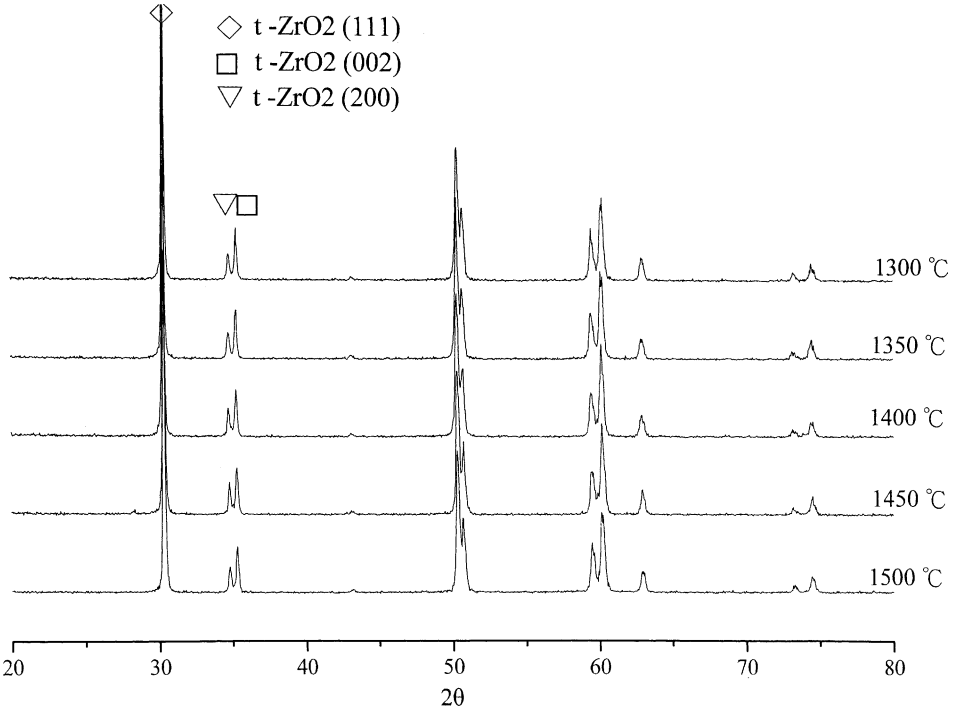

Fig. 6. X-ray spectra of samples at different sintering temperatures.

with the heating rate of 5 °C/min started at about 1100 °C and completed at about 1300 °C and had the largest shrinkage. This is because the sample with lower heating rate could absorb more energy to help pores diffuse out to the surface resulting in a higher densification than other samples. Thus, a larger shrinkage was observed at a heating rate of 5 °C/min. The linear shrinkages of the samples with heating rates of 5, 10, 20 °C/min were 22, 18, 17%, respectively. For samples with the heating rates of 10 and 20 °C/min, the shrinkage onset temperatures were shifted to 1125 and 1150 °C, and the densification completed at 1325 and 1350 °C, respectively. The temperature in which the maximum shrinkage rate occurred was shifted to a higher temperature and the maximum shrinkage decreased with increasing heating rate of 3-YE samples.

3.2. Activation energy analysis

The activation energy of the early-stage sintering of Y-TZP is based on the work of Tianshu et al. [8] The relationship between $(\Delta L/L_0)_T$ and the heating rate, C, during early-stage sintering can be expressed as

$$\ln\left(\frac{\Delta L}{L_0}\right) = -\frac{\ln C}{m+1} \quad (1)$$

Based on Eq. (1), the slope of natural logarithm of relative shrinkage at a particular temperature, $(\Delta L/L_0)_T$,

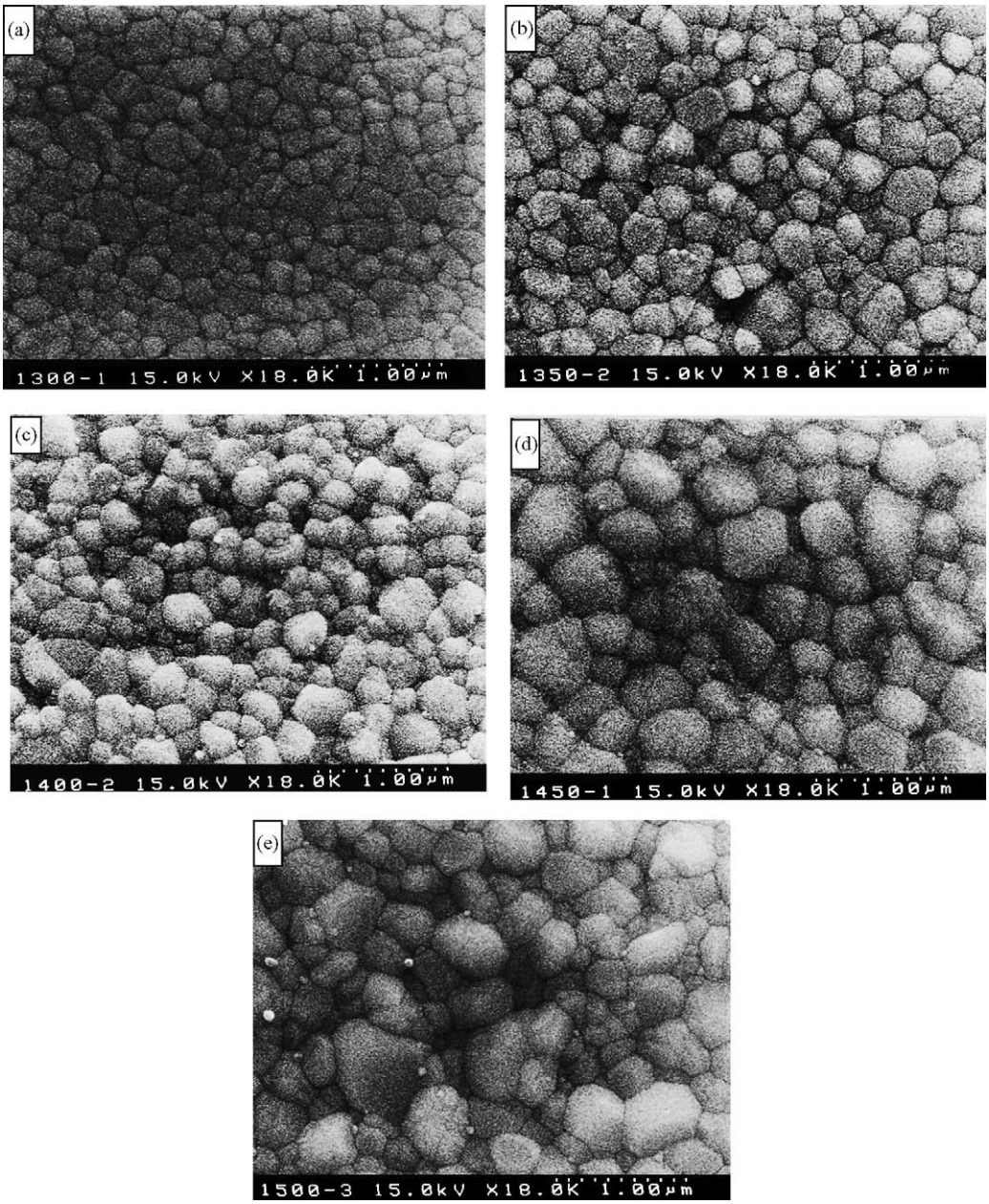

Fig. 7. SEM micrographs of samples sintered at different temperatures: (a) 1300 °C, (b) 1350 °C, (c) 1400 °C, (d) 1450 °C, (e) 1500 °C.

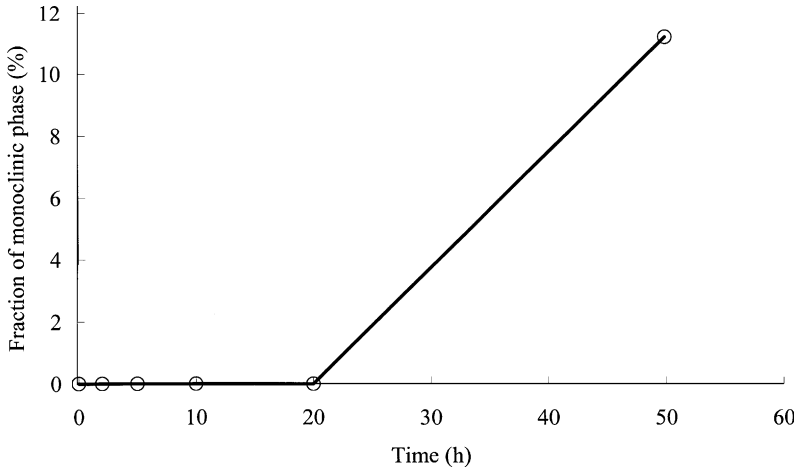

Fig. 8. The fraction of monoclinic phase formed as a function of aging time during aging in water at 100 °C for samples sintered at 1500 °C.

against heating rate, C, can be obtained. Then, one can derive the early-stage diffusion mechanism developed by Young and Culter [9]. The values of m represent the early-stage diffusion mechanisms, i.e. $m = 0$ for viscous flow, $m = 1$ for volume diffusion and $m = 2$ for grain boundary diffusion mechanisms. Fig. 3 was plotted according to the 3-YE shrinkage curve and the equation of early-stage sintering mechanism [8]. The average value of m for 3-YE obtained from Fig. 3 and Eq. (1) is 1 which shows that the early-stage diffusion mechanism was controlled by volume diffusion for 3-YE.

Based on the kinetic equation of non-isothermal sintering [9]

$$\ln\left(\frac{\mathrm{d}\rho}{\mathrm{d}t}T\right) = \frac{-Q}{RT} \tag{2}$$

where ρ is the density and Q is the activation energy of early-stage sintering. Fig. 4 shows the plots of $\ln((\mathrm{d}\rho/\mathrm{d}t)T)$ versus $1/T$ under the non-isothermal sintering condition according to Eq. (2). The values of the activation energy can be calculated by substituting the slope of each plot into Eq. (2).

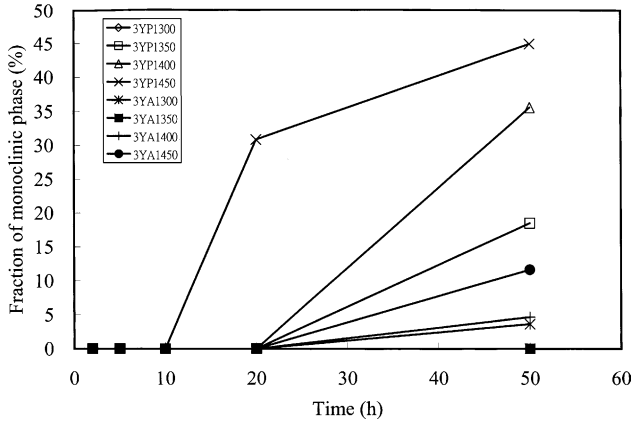

Fig. 9. The fraction of monoclinic phase formed as a function of aging time during aging in water at 100 °C for polished (3YP) and annealed (3YA) samples sintered at different temperatures.

The calculated value of the activation energy for 3-YE is about 643 ± 43 kJ/mol (Fig. 5), which agrees well with the value of 615 ± 70 kJ/mol proposed by Wang and Raj [10] during early-stage sintering. It also agrees well with the average creep activation energy of Y-TZP (650 ± 70 kJ/mol) that has ever been proposed [11].

3.3. Crystalline phase

Fig. 6 shows the X-ray diffraction patterns of the samples sintered at different temperatures, indicating only t phase present in the sintered bodies. However, the broadening phenomena of t phase (1 1 1) plane in specimens that were sintered above 1450 °C were also observed. This may be due to the solute partition of Y_2O_3 resulting from the long soaking time at a high temperature, which resulted in the formation of Y_2O_3-rich big grains (c phase) and Y_2O_3-poor small grains (t phase). The angle of $(1\ 1\ 1)_c$ and $(1\ 1\ 1)_t$ are pretty close ($2\theta = 30.17$ and 30.368°, respectively), and is the main reason for causing asymmetrical X-ray peak broadening phenomenon.

3.4. Grain size and microstructure

Fig. 7 shows the microstructures of the sintered Y-TZP. The grain sizes of the samples sintered at 1300, 1350, and 1400 °C were uniform and were 214, 221, and 289 nm, respectively. As the sintering temperature increased to 1450 and 1500 °C, the partial big grains (470 and 714 nm) which spread in small grains (300 and 431 nm) were observed. This may result from the solute partition of Y_2O_3.

3.5. Low temperature degradation

No m phase was observed in the specimens after low temperature (100 °C) aging for 50 h, except for the specimen sintered at 1500 °C. Fig. 8 shows the change in the fraction of monoclinic phase as a function of aging time for 3-YE YTZP specimens sintered at 1500 °C. It is believed that

yttria used to stabilize t-ZrO_2 grains was segregated for the sample sintered at 1500 °C. This reduced the amount of yttria in some t phase grains resulting in the grain growth of t phase grains. Then, the m phase was formed from the grains that are close to the critical grain size, which resulted in lowering the ability of the anti-LTD.

Fig. 9 shows the change in the fraction of monoclinic phase as a function of aging time for 3-YE polished and annealed Y-TZP specimens sintered at different temperatures. It is observed that the amount of m phase increased upon increasing the aging time and sintering temperature. The LTD behavior is primarily dominated by the grain size at lower sintering temperatures. This is because the solute partition of Y_2O_3 would not occur at the lower sintering temperatures, so the Y_2O_3 content in each grain was almost the same. However, the t → m phase transformation induced by the grain growth occurred easily as the sintering temperature increased, which resulted in the poor anti-LTD ability. This can be seen easily in the samples sintered at temperatures above 1450 °C. The Y_2O_3 content in the t phase grain became lower due to the occurrence of solute partition and, correspondingly the anti-LTD property decreased. Thus, the m phase would increase rapidly as the aging time increased.

The onset time of the occurrence of m-ZrO_2 in the annealed samples during LTD was longer than the unannealed samples (Fig. 9). For the sample sintered at 1450 °C, the onset time of the occurrence of m-ZrO_2 is retarded from 10 to 20 h after annealing. This may be because Y_2O_3 became enriched at the grain boundary and the surface after annealing, which stabilized the t phase grains near the surface and grain boundary. This resulted in a better anti-LTD property which agrees well with the proposed results of Lance et al. [12].

4. Conclusion

The calculated value of the activation energy for 3-YE in this experiment is about 643 ± 43 kJ/mol during the early-stage sintering.

It was found that the solute partition of Y_2O_3 occurred when the sintering temperature increased to 1450 and 1500 °C.

The LTD behavior was primarily dominated by the grain size at lower sintering temperatures, and the solute partition amount of yttria at higher temperatures. Besides, the annealing treatment yielded a better anti-LTD property.

References

[1] F.F. Lange, Transformation-toughened ZrO_2: correlations between grain size control and composition in the system ZrO_2–Y_2O_3, J. Am. Ceram. Soc. 69 (3) (1986) 240–242.
[2] R.A. Kimel, J.H. Adair, Aqueous degradation and chemical passivation of yttria-tetragonally-stabilized zirconia at 25 °C, J. Am. Ceram. Soc. 85 (6) (2002) 1403–1408.
[3] J.F. Li, R. Watanabe, Influence of a small amount of Al_2O_3 addition on the transformation of Y_2O_3-partially stabilized ZrO_2 during annealing, J. Mater. Sci. 32 (1997) 1149–1153.
[4] X. Guo, Low temperature degradation mechanism of tetragonal zirconia ceramics in water: role of oxygen vacancies, Solid State Ionics 112 (1998) 113–116.
[5] H.C. Kao, F.Y. Ho, C.C. Yang, W.J. Wei, Surface machining of fine-grain Y-TZP, J. Eur. Ceram. Soc. 20 (2000) 2447–2455.
[6] C.C. Yang, W.J. Wei, Effects of material properties and testing parameters on wear properties of fine-grain zirconia, Wear 242 (2000) 97–104.
[7] S.N.B. Hodgson, J. Cawley, M. Clubley, The role of Al_2O_3 impurities on the microstructure and properties of Y-TZP, J. Mater. Process. Tech. 92–93 (1999) 85–90.
[8] Z. Tianshu, P. Hing, H. Huang, Early-stage sintering mechanisms of Fe-doped CeO_2, J. Mater. Sci. 37 (2002) 997–1003.
[9] W.S. Young, I.B. Culter, Initial sintering with constant rates of heating, J. Am. Ceram. Soc. 53 (12) (1970) 659–663.
[10] J. Wang, R. Raj, Activation energy for the sintering of two-phase alumina/zirconia ceramics, J. Am. Ceram. Soc. 74 (8) (1991) 1959–1963.
[11] D.M. Owen, A.H. Chokshi, Final stage free sintering and sinter forging behavior of a yttria-stabilized tetragonal zirconia, J. Am. Ceram. Soc. 46 (2) (1998) 719–729.
[12] M.J. Lance, E.M. Vogel, L.A. Rieth, W.R. Cannon, Low-temperature aging of zirconia ferrules for optical connectors, J. Am. Ceram. Soc. 84 (11) (2001) 2731–2733.